THE GEOLOGICAL SOCIETY OF AMERICA®

East African weathering dynamics controlled by vegetation-climate feedbacks

Sarah J. Ivory[1], Michael M. McGlue[2], Geoffrey S. Ellis[3], Adam Boehlke[3], Anne-Marie Lézine[4], Annie Vincens[5], and Andrew S. Cohen[6]
[1]Department of Earth, Environment, and Planetary Sciences, Brown University, Providence, Rhode Island 02912, USA
[2]Department of Earth and Environmental Sciences, University of Kentucky, Lexington, Kentucky 40506, USA
[3]Central Energy Resources Science Center, U.S. Geological Survey, Denver, Colorado 80226, USA
[4]Laboratoire d'Océanographie et du Climat (LOCEAN), CNRS, 75005 Paris, France
[5]Centre de Recherche et d'Enseignement de Géosciences (CEREGE), CNRS, 13545 Aix-en-Provence cedex 4, France
[6]Department of Geosciences, University of Arizona, Tucson, Arizona 85721, USA

ABSTRACT

Tropical weathering has important linkages to global biogeochemistry and landscape evolution in the East African rift. We disentangle the influences of climate and terrestrial vegetation on chemical weathering intensity and erosion at Lake Malawi using a long sediment record. Fossil pollen, microcharcoal, particle size, and mineralogy data affirm that the detrital clays accumulating in deep water within the lake are controlled by feedbacks between climate and hinterland forest composition. Particle-size patterns are also best explained by vegetation, through feedbacks with lake levels, wildfires, and erosion. We develop a new source-to-sink framework that links lacustrine sedimentation to hinterland vegetation in tropical rifts. Our analysis suggests that climate-vegetation interactions and their coupling to weathering/erosion could threaten future food security and has implications for accurately predicting petroleum play elements in continental rift basins.

INTRODUCTION

Weathering affects all biogeochemical cycles and is key to critical zone dynamics. Weathering has been shown to impact soil stability, with potential effects on carbon transport, sediment loading, and nutrient cycling. On human time scales, weathering changes may place fisheries and potable water supplies at risk of sediment pollution. On longer (10^5–10^7 yr) time scales, these processes link rock decay and sediment transport in hinterlands with stratal development in basins, and underpin source-to-sink sedimentary models (Romans et al., 2015). Thus, knowledge of weathering and erosion patterns across different time scales provides a framework for many applications.

The importance of modern biosphere-geosphere interactions on weathering has been highlighted in experimental watershed studies (Dunne, 1979; Drever, 1994; Berner and Cochran, 1998). For example, interactions between biotic and abiotic systems have been studied at the Luquillo Critical Zone Observatory (Puerto Rico) (e.g., White et al., 1998). However, the Luquillo forest is an end-member tropical landscape and may not be broadly applicable to other environments. Further, observational records are commonly too short to capture information relevant to global change or source-to-sink problems in ancient basins (Einsele and Hinderer, 1998). By contrast, most studies of deep-time weathering have focused on feedbacks with climate or orogenesis (Lee et al., 2015), and the lack of long vegetation records biases models that incorporate climate alone. Moreover, paleoecological records suggest that climate plays an indirect role mediated through vegetation change (Ivory et al., 2014). Thus, biologically mediated weathering has been called the most "provocative, important, and testable" hypothesis of the next decade (Brantley et al., 2011, p. 141). This same problem was identified by the basin analysis community, as a lack of paleovegetation data limits the accuracy of predictive sediment modeling (Heins and Kairo, 2007).

Herein we use multiple proxies from Lake Malawi drill cores to examine the relationships among climate, vegetation, and sedimentation beginning at ca. 100 ka (Ivory et al., 2016). As Lake Malawi watershed vegetation is sensitive to changes in both rainfall and seasonality, the integration of sedimentological and pollen data affords an opportunity to investigate weathering patterns in response to rainfall amount and vegetation semi-independently.

BACKGROUND

Bedrock at Lake Malawi is dominated by Proterozoic basement with localized outcrops of Cenozoic volcanic and Mesozoic sedimentary rocks (Fig. 1; Persits et al., 1997). Lowland soils are pellic vertisols and mollic andosols, whereas the mountains have lithosols, chromic cambisols, and dystric regosols (United Nations Food and Agriculture Organization, 1998). The lake is situated at the southern limit of the Intertropical Convergence Zone. Mean annual precipitation (MAP) has a strongly decreasing north-south gradient, ranging from 2400 to 800 mm/yr, with a single November–April rainy season.

Modern sediments are dominantly medium- to fine-grained sands within 1–2 km of deltas, and finer particles occur at >30 m depth (Dolozi et al., 2011). However, coarse-grained sediments are found in all depositional environments due to gravity flows (Soreghan et al., 1999). Clay mineralogy studies show smectite, kaolinite, and illite present, in rank order, with an increase in smectite southward, suggesting a linkage between dry climate and smectite abundance (Kalindekafe et al., 1996).

Vegetation is largely constrained by rainfall and rainfall seasonality (Ivory et al., 2014). Open-canopy Zambezian miombo woodlands grow in areas of highly seasonal rainfall. Closed-canopy tropical seasonal forests occur in areas with a shorter dry season and moister edaphic conditions. Above 1500 m above sea level (asl), closed-canopy Afromontane forests are dominant with high-elevation grasslands (White, 1983).

METHODS

A previous study from Lake Malawi showed that vegetation and fire frequency were strong controls on chemical weathering and erosion (Ivory et al., 2014). However, it is unknown if these processes differ over multiple climate cycles. To investigate these relationships, we used fossil pollen, terrigenous grain size, and clay minerals from core MAL05-1B (11°18′S, 34°26′E; 359 m depth; Fig. 1). This ~90 k.y., 52 m interval (62–114 m below lake floor [mblf]) was divided into parasequences based on lithofacies stacking patterns (see the GSA Data Repository[1] for methods).

[1]GSA Data Repository item 2017277, methods, and supplemental Figures DR1–DR3, is available online at http://www.geosociety.org/datarepository/2017/ or on request from editing@geosociety.org.

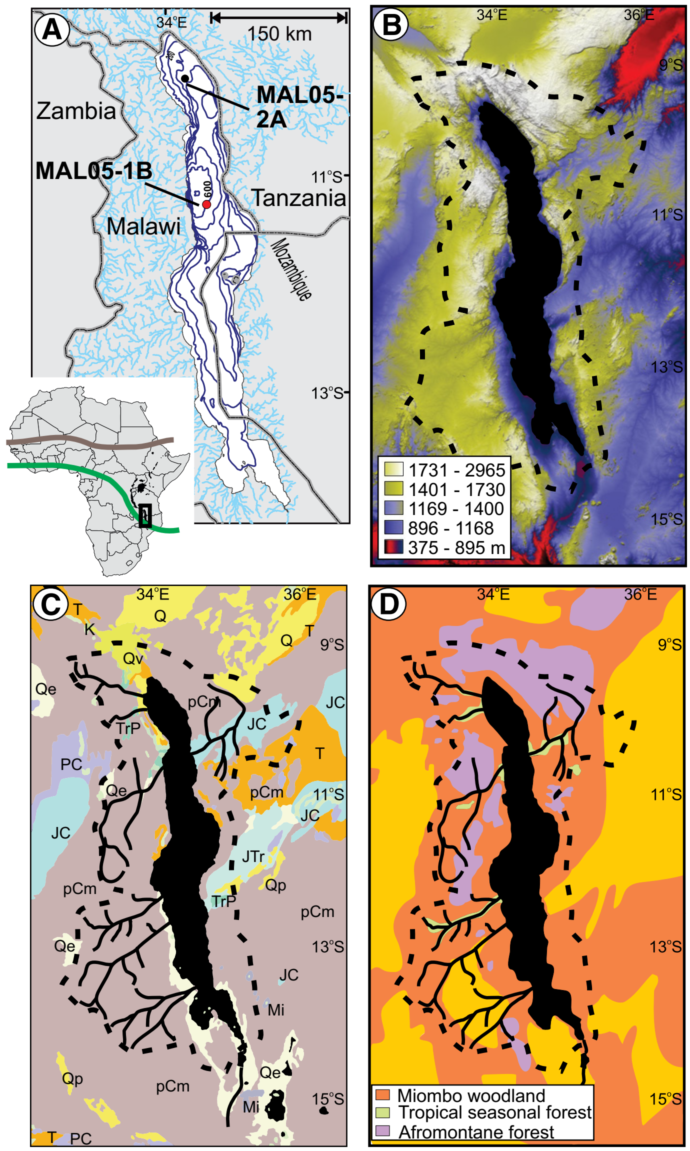

Figure 1. Maps of study area, Lake Malawi, East Africa. Inset shows map of Africa showing study site (black rectangle) and location of Intertropical Convergence Zone (ITCZ) in January (green) and July (brown). A: Bathymetry. Lake Malawi drill cores are indicated with dots. B: Topography. C: Bedrock geology (Persits et al., 1997). D: Modern vegetation. Geologic map units: Q—Quaternary; Qe—Holocene; Qp—Pleistocene; Qv—Quaternary igneous; T—Tertiary; K—Cretaceous; JTr—Jurassic and Triassic; Mi—Mesozoic igneous; JC—Jurassic–Carboniferous; TrP—Triassic–Permian; PC—Permian–Carboniferous; pCm—Precambrian.

Over the studied interval, three parasequences occur that represent cyclic lake-level change (Fig. 2). Parasequence one (P1), the oldest lake cycle, occurs from 114 to 90 mblf (180–140 ka), parasequence two (P2) from 90 to 77 mblf (140–123 ka), and parasequence three (P3) from 77 to 62 mblf (123–93 ka). The core age model suggests that the Penultimate Glacial–Last Interglacial transition occurs at the end of P2, thus only P3 occurs during the Last Interglacial (Ivory et al., 2016).

RESULTS AND DISCUSSION

Long-Term Weathering and Vegetation

The vegetation record displays trends that are mirrored in the parasequences. Profundal lithofacies at each parasequence base are coeval with

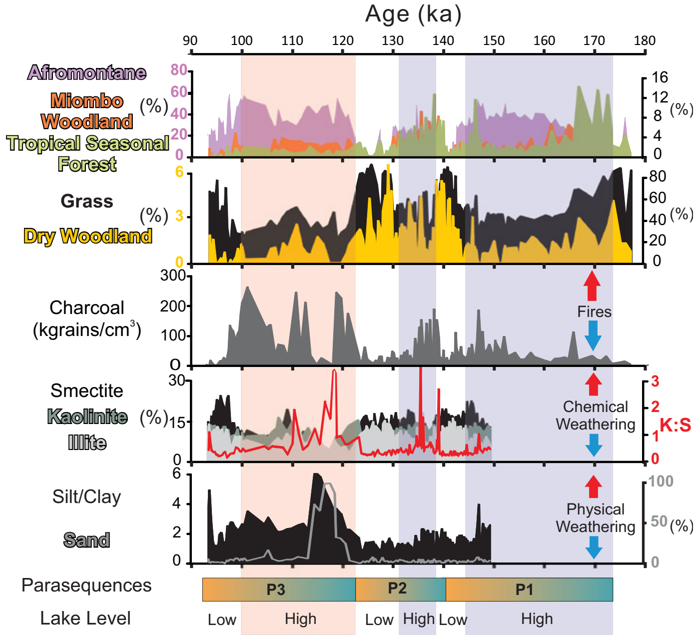

Figure 2. Vegetation and weathering indicators from core MAL05-1B, Lake Malawi, East Africa. Purple axis and curve corresponds to abundances of afromontane forest pollen; right-side black axis shows for pollen abundances of all other vegetation types. Weathering indicators are normalized clay mineral percentages and ratio of kaolinite:smectite (K:S; red line). Red and blue shading indicate three highstands that differ based on rainfall seasonality, with red for long dry season, and blue for short dry season.

forest phases (Fig. 2; Fig. DR1 in the Data Repository). The upper portions of the parasequences consist of shallow-water lithofacies and semi-arid vegetation. The data suggest that forest expansion occurred when rainfall was high (100% of modern; Lyons et al., 2011) and the lake was at highstand. Very reduced rainfall (–61% less than modern) resulted in regression and replacement by discontinuous semi-arid bushland (Fig. 2). Thus, three forest expansion and retreat cycles are recorded.

Forest composition during wet periods differs in each parasequence. During the P1 and P2 forest phases, occurring during the penultimate glacial, highland and lowland forest, as well as miombo woodland, were abundant (Fig. 2). In contrast, during P3, only highland forest and miombo woodland expanded, suggesting more open lowland vegetation. Previous work has documented similar assemblages when MAP was near modern but the dry season length was ~6 mo, suggesting that a seasonality change resulted in the different P3 vegetation composition (Ivory et al., 2014).

Low charcoal concentrations suggest infrequent fires during all semi-arid phases (Fig. 2). Similar ecosystems today show infrequent fires despite aridity as a result of discontinuous vegetation (Makishima, 2005). Although charcoal concentrations are higher during all forest phases, maximum values occurred only during the P3 forest phase, when open woodland dominated.

Clay minerals in the strata consist of smectite, kaolinite, illite, and chlorite, in rank order. Kaolinite, a leaching indicator, reached high values (≥15% of clays) during highstands. By contrast, smectite, common in less-altered tropical soil profiles, reached high percentages during lowstands (Fig. 2). This pattern was especially clear in P3, where smectite was routinely >25% in lowstand sediments. The highest kaolinite to smectite ratio occurred in P2, suggesting very intense chemical weathering (Pastouret et al., 1978). Much less variability is present in illite, associated with strong physical weathering, although the highest values occurred during the P3 and P2 lowstands (Hillier, 1995).

Detrital grain size provides indications of storage release from deltas, hinterland transport distance, and sub-lacustrine depositional processes

(Ivory et al., 2014). With the exception of a thicker (~128 cm) mass-wasting deposit at the base of P3 and two thin turbidites in P2, sand content is low. A high silt:clay ratio occurs at each parasequence base, although coarsening varied. P3 contained the coarsest profundal lithofacies (mean silt:clay of 2.9), whereas the silt:clay in P1 and P2 was lower (Fig. 2). A trait common to all three parasequences was that lowstand lithofacies contained very fine-grained sediments.

Conceptual Model of Vegetation and Weathering

Our data suggest that on long time scales, variations in chemical weathering intensity are not adequately explained by rainfall or temperature alone. Water levels at Lake Malawi respond to effective precipitation, resulting in parasequence development (Fig. 2; Fig. DR2). If temperature or rainfall were the most direct control on weathering, the parasequence clay minerals should mirror the wet-dry cycles. Although all lowstands share indications of reduced chemical weathering, clay mineral variability during the highstands suggests differing critical zone dynamics. The kaolinite contents during the P2 (~14.4% ± 5%) and P1 (~13.0% ± 5%) highstands were relatively high in comparison to that of the P3 highstand (~11.4% ± 5%). As the P2-P3 boundary is associated with a glacial-interglacial transition, if weathering were strongly controlled by rainfall and temperature, higher temperatures and monsoon enhancement over the transition should increase chemical weathering. However, kaolinite concentrations are greater during the cooler and/or drier glacial parasequences.

Instead, we interpret forest composition as a critical control on weathering intensity. During the P1 and P2 highstands, dense lowland and highland forest was present as a result of high rainfall and low seasonality. In contrast, during P3, a long dry season limited lowland forest expansion. In modern forested watersheds, vegetation density and composition are linked to organic acid abundance in soils, which catalyzes chemical reactions leading to rapid aluminosilicate breakdown (Blum et al., 2002). The link between vegetation and weathering is further supported by high abundances of smectite and grass pollen, as well as low silt:clay, in lowstand deposits, indicating that opening of the lowland landscape reduces leaching and sediment transport (Fig. 2).

The grain-size pattern is also best explained by linkages to vegetation composition. Highest silt:clay values are recorded during highstand forest phases (Fig. 2). Furthermore, there are differences in grain size among highstands, such that the P3 highstand exhibits higher average silt:clay. This suggests that open woodland is more conducive to sediment flushing, as less rainfall is intercepted by the canopy. Furthermore, reduced root networks are less effective at retaining infiltrated moisture (Roering et al., 2010). Thus, seasonal rivers with flashy discharge transport sediment-laden water to deltas, which transforms into hyperpycnal flows capable of delivering a high silt:clay sediment to deep water. A similar mechanism is responsible for transporting terrestrial organic matter to deepwater environments (Ellis et al., 2015).

Further, we observe differences among the style of deposition in P2 and P3. Posamentier and Kolla (2003) noted that regressions, steep slopes, and sand in shelf-margin staging areas are prerequisites for sand in deep-water marine settings. At Lake Malawi, our stratal record indicates that gravity flows occurred during lake level highstands. It is plausible that a threshold was crossed from P2 to P3 that provided the conditions necessary to explain the coarser grain-size trend. We suggest that this threshold was a change to strong rainfall seasonality that altered both vegetation and fluvial dynamics. By analogy, Fraticelli (2006) observed that delta progradation along the Texas (USA) coast occurred when severe droughts denuded coastal-plain vegetation preceding major floods. The P2 littoral deposits mark an important transition in the record. This transition conditioned a change in weathering and erosion, which is unequivocally the result of the establishment of open miombo woodlands.

Wildfires were most associated with open woodlands (Fig. 2). Micro-charcoal abundances in P1 and P2 suggest only modest fire activity, consistent with abundant evergreens, suggesting that fire is not a key feedback on erosion during these intervals. In contrast, fires served as a strong positive feedback on sediment flushing in P3. Wildfires destroy root networks and reduce hillslope stability, leading to higher occurrences of post-fire debris flows and sediment yields (Moody et al., 2013).

These trends are confirmed by a principal components analysis, which shows covariance between vegetation and sedimentology (see the Data Repository), and are in agreement with patterns in a shorter Lake Malawi record (Ivory et al., 2014). Combining these data sets, we constructed a conceptual model describing patterns of vegetation-weathering-climate interactions (Fig. 3). Tree expansion occurred when rainfall was high. However, lowland forest occurs only during short dry seasons, while woodland predominates during longer dry seasons. Although woodland and lowland forest occur under similar total rainfall, dense forests lead to reduced wildfires, more intense chemical weathering, and moderately silty detritus. When long dry seasons preclude dense forests, the open vegetation is amenable to variable weathering and common fires, which condition the landscape for mass wasting and sand/silt in deep water. When rainfall is low, discontinuous semi-arid vegetation is fuel limited, resulting in few fires. The sparse vegetation leads to fine detrital sediments that are smectite and illite rich, suggesting limited chemical weathering and sediment transport.

CONCLUSIONS AND IMPLICATIONS

We show that feedbacks between vegetation and climate are critically important to weathering and erosion. In studies of both deep-time and modern watersheds, it is clear that sediment generation, erosion, and phytogeography are complexly linked (Torres-Acosta et al., 2015). We demonstrate that across Quaternary time scales, a strong influence of vegetation composition and structure on weathering intensity exists that has far-reaching implications.

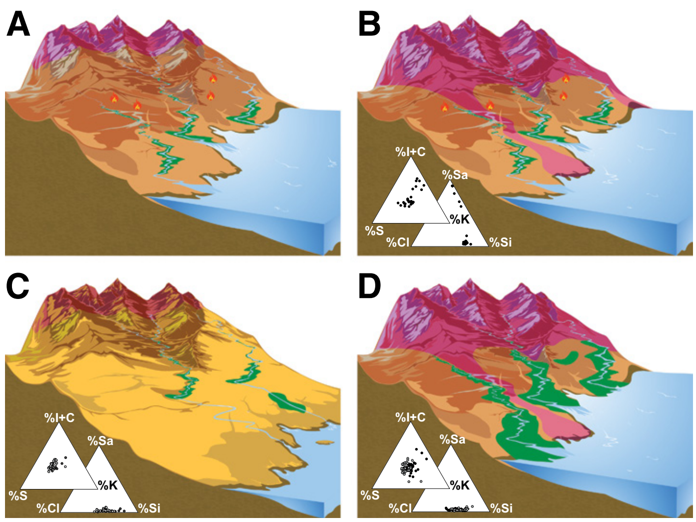

Figure 3. Conceptual source-to-sink model for vegetation change in a tropical lacustrine rift setting. Purple—afromontane forest; orange—miombo woodland; yellow—semi-arid vegetation; green—tropical lowland forest. Ternary diagrams reflect clay mineralogy (K–[I + C]–S) (where K is kaolinite, I is illite, C is chlorite, and S is smectite) and detrital particle size (Si-Sa-Cl) data. A: Modern setting. B: Presence of open woodland where many wildfires result in reduced chemical weathering and delivery of less weathered clay minerals to lake and prime landscape for erosion. C: Arid intervals with expansion of desert ecosystems resulting in deposition of fine-grained sediments and less chemically altered clays (gray points—arid intervals; black points—megadrought interval). D: Expansion of lowland forest resulting in increased chemical weathering and deposition of more altered clay minerals (gray points— parasequence one (P1); black points—P2).

First, these interactions could impact future sustainable development. For example, at Lake Tanganyika (East Africa), sediment pollution alters the aquatic food web and the potential for healthy fish yields, which are relied upon for protein and income (Cohen et al., 2016). Today most paleo-environmental studies consider climate change as the primary driver of weathering regime alteration (Harris and Mix, 1999). However, if vegetation and climate have a complex interdependence, it will be critical to consider both aspects in developing management strategies, particularly when land use decouples vegetation from climate.

On geological time scales, tropical rifts are an important component of the global petroleum endowment. Productivity, preservation, and dilution are the key controls on developing petroleum source rocks (Bohacs et al., 2000). Our results indicate that dilution of organic-rich profundal sediments could be affected by hinterland vegetation patterns in rifts. Higher silt:clay could impact source-rock quality for conventional and unconventional systems (Katz and Lin, 2014). These data also suggest that the accuracy of sediment composition forward models used for reservoir prediction hinges on accounting for vegetation dynamics (Heins and Kairo, 2007).

ACKNOWLEDGMENTS

We thank the U.S. National Science Foundation (grant EAR-0602404), the U.S. Geological Survey, and the American Chemical Society–Petroleum Research Fund program (54376-DNI8) for funding. Thanks to W. Benzel for analytical assistance, and LacCore at the University of Minnesota for core curation. We also thank the anonymous reviewers who helped improve this manuscript.

REFERENCES CITED

Berner, R.A., and Cochran, M.F., 1998, Plant-induced weathering of Hawaiian basalts: Journal of Sedimentary Research, v. 68, p. 723–726, doi:10.2110/jsr.68.723.

Blum, J.D., Klaue, A., Nezat, C.A., Driscoll, C.T., Johnson, C.E., Siccama, T.G., Eagar, C., Fahey, T.J., and Likens, G.E., 2002, Mycorrhizal weathering of apatite as an important calcium source in base-poor forest ecosystems: Nature, v. 417, p. 729–731, doi:10.1038/nature00793.

Bohacs, K.M., Carroll, A.R., Neal, J.E., and Mankiewicz, P.J., 2000, Lake-basin type, source potential, and hydrocarbon character: An integrated sequence-stratigraphic geochemical framework, *in* Gierlowski-Kordesch, E.H., and Kelts, K.R., eds., Lake Basins Through Space and Time: American Association of Petroleum Geologists Studies in Geology 46, p. 3–34.

Brantley, S.L., et al., 2011, Twelve testable hypotheses on the geobiology of weathering: Geobiology, v. 9, p. 140–165, doi:10.1111/j.1472-4669.2010.00264.x.

Cohen, A.S., Gergurich, E.L., Kraemer, B., McGlue, M.M., McIntyre, P., Russell, J.M., Simmons, J., and Swarzenski, P., 2016, Climate warming reduces fish production and benthic habitat in Lake Tanganyika, one of the most biodiverse freshwater ecosystems: Proceedings of the National Academy of Sciences of the United States of America, v. 113, p. 9563–9568, doi:10.1073/pnas.1603237113.

Dolozi, M.B., Kalindekafe, L.S., Ngongondo, C., and Dulanya, Z., 2011, A comparative analysis of the distribution, composition and geochemistry of surface sediments in the Linthipe and Songwe River Deltas of Lake Malawi: Journal of African Earth Sciences, v. 60, p. 93–105, doi:10.1016/j.jafrearsci.2011.02.002.

Drever, J.I., 1994, The effect of land plants on weathering rates of silicate minerals: Geochimica et Cosmochimica Acta, v. 58, p. 2325–2332, doi:10.1016/0016-7037(94)90013-2.

Dunne, T., 1979, Sediment yield and land use in tropical catchments: Journal of Hydrology (Amsterdam), v. 42, p. 281–300, doi:10.1016/0022-1694(79)90052-0.

Einsele, G., and Hinderer, M., 1998, Quantifying denudation and sediment-accumulation systems (open and closed lakes): Basic concepts and first results: Palaeogeography, Palaeoclimatology, Palaeoecology, v. 140, p. 7–21, doi:10.1016/S0031-0182(98)00041-8.

Ellis, G.S., Katz, B.J., Scholz, C.A., and Swart, P.K., 2015, Organic sedimentation in modern lacustrine systems: A case study from Lake Malawi, East Africa, *in* Larsen, D., et al., eds., Paying Attention to Mudrocks: Priceless!: Geological Society of America Special Paper 515, p. 19–47, doi:10.1130/2015.2515(02).

Fraticelli, C.M., 2006, Climate forcing in a wave-dominated delta: The effects of drought–flood cycles on delta progradation: Journal of Sedimentary Research, v. 76, p. 1067–1076, doi:10.2110/jsr.2006.097.

Harris, S.E., and Mix, A.C., 1999, Pleistocene precipitation balance in the Amazon Basin recorded in deep sea sediments: Quaternary Research, v. 51, p. 14–26, doi:10.1006/qres.1998.2008.

Heins, W.A., and Kairo, S., 2007, Predicting sand character with integrated genetic analysis, *in* Arribas, J., et al., eds., Sedimentary Provenance and Petrogenesis: Perspectives from Petrography and Geochemistry: Geological Society of America Special Paper 420, p. 345–379, doi:10.1130/2006.2420(20).

Hillier, S., 1995, Erosion, sedimentation and sedimentary origin of clays, *in* Velde, B., ed., Origin and Mineralogy of Clays: Berlin, Springer, p. 162–219, doi:10.1007/978-3-662-12648-6_4.

Ivory, S.J., McGlue, M.M., Ellis, G.S., Lézine, A.M., Cohen, A.S., and Vincens, A., 2014, Vegetation controls on weathering intensity during the last deglacial transition in southeast Africa: PLoS One, v. 9, e112855, doi:10.1371/journal.pone.0112855.

Ivory, S.J., Blome, M.W., King, J., McGlue, M.M., Cole, J., and Cohen, A.C., 2016, Paleoecology links climate change and landscape dynamics with adaptive radiation of cichlids at Lake Malawi: Proceedings of the National Academy of Sciences of the United States of America, v. 113, p. 11,895–11,900, doi:10.1073/pnas.1611028113.

Kalindekafe, L.N., Dolozi, M.B., and Yuretich, R., 1996, Distribution and origin of clay minerals in the sediments of Lake Malawi, *in* Johnson, T.C., and Odada, E., eds., The Limnology, Climatology and Paleoclimatology of the East African Lakes: Amsterdam, Gordon and Breach, p. 443–460.

Katz, B., and Lin, F., 2014, Lacustrine basin unconventional resource plays: Key differences: Marine and Petroleum Geology, v. 56, p. 255–265, doi:10.1016/j.marpetgeo.2014.02.013.

Lee, C.T.A., Thurner, S., Paterson, S., and Cao, W., 2015, The rise and fall of continental arcs: Interplays between magmatism, uplift, weathering, and climate: Earth and Planetary Science Letters, v. 425, p. 105–119, doi:10.1016/j.epsl.2015.05.045.

Lyons, R.P., Scholz, C.A., Buoniconti, M.R., and Martin, M.R., 2011, Late Quaternary stratigraphic analysis of the Lake Malawi Rift, East Africa: An integration of drill-core and seismic-reflection data: Palaeogeography, Palaeoclimatology, Palaeoecology, v. 303, p. 20–37, doi:10.1016/j.palaeo.2009.04.014.

Makishima, H., 2005, Flora and vegetation of Nachola, Samburu District, northern Kenya: A study of vegetation in an arid land: African Study Monographs, v. 32, Supplement, p. 63–78.

Moody, J.A., Shakesby, R.A., Robichaud, P.R., Cannon, S.H., and Martin, D.A., 2013, Current research issues related to post-wildfire runoff and erosion processes: Earth-Science Reviews, v. 122, p. 10–37, doi:10.1016/j.earscirev.2013.03.004.

Pastouret, L., Chamley, H., Delibrias, G., Duplessy, J.C., and Thiede, J., 1978, Late Quaternary climatic changes in western tropical Africa deduced from deep-sea sedimentation off the Niger delta: Oceanologica Acta, v. 1, p. 217–232.

Persits, F.M., Ahlbrandt, T.S., Tuttle, M.L., Charpentier, R.R., Brownfield, M.E., and Takahashi, K., 1997, Maps showing geology, oil and gas fields and geological provinces of Africa: U.S. Geological Survey Open-File Report 97-470-A.

Posamentier, H.W., and Kolla, V., 2003, Seismic geomorphology and stratigraphy of depositional elements in deep-water settings: Journal of Sedimentary Research, v. 73, p. 367–388, doi:10.1306/111302730367.

Roering, J.J., Marshall, J., Booth, A.M., Mort, M., and Jin, Q., 2010, Evidence for biotic controls on topography and soil production: Earth and Planetary Science Letters, v. 298, p. 183–190, doi:10.1016/j.epsl.2010.07.040.

Romans, B.W., Castelltort, S., Covault, J.A., Fildani, A., and Walsh, J.P., 2015, Environmental signal propagation in sedimentary systems across timescales: Earth-Science Reviews, v. 153, p. 7–29, doi:10.1016/j.earscirev.2015.07.012.

Soreghan, M.J., Scholz, C.A., and Wells, J.T., 1999, Coarse-grained, deep-water sedimentation along a border fault margin of Lake Malawi, Africa: Seismic stratigraphic analyses: Journal of Sedimentary Research, v. 69, p. 832–846, doi:10.2110/jsr.69.832.

Torres Acosta, V., Bande, A., Sobel, E.R., Parra, M., Schildgen, T.F., Stuart, F., and Strecker, M.R., 2015, Cenozoic extension in the Kenya Rift from low-temperature thermochronology: Links to diachronous spatiotemporal evolution of rifting in East Africa: Tectonics, v. 34, p. 2367–2386, doi:10.1002/2015TC003949.

United Nations Food and Agriculture Organization, 1988, Soil map of the World, Revised legend: United Nations Food and Agriculture Organization World Soil Resources Report 60, scale 1:5,000,000.

White, A.F., Blum, A.E., Schulz, M.S., Vivit, D.V., Stonestrom, D.A., Larsen, M.C., Murphy, S.F., and Eberl, D., 1998, Chemical weathering in a tropical watershed, Luquillo Mountains, Puerto Rico: I. Long-term versus short-term weathering fluxes: Geochimica et Cosmochimica Acta, v. 62, p. 209–226, doi:10.1016/S0016-7037(97)00335-9.

Manuscript received 4 January 2017
Revised manuscript received 4 May 2017
Manuscript accepted 5 May 2017

Printed in USA